Study of the Shoulder Response to a High Speed – Short Displacement Lateral Impact using Post Mortem Human Subjects and ES-2re dummy.

M. Lebarbé, D. Lafont, J. Uriot, P. Potier, P. Baudrit, G. Vallencien

Abstract A specific test setup was designed to recreate in a laboratory the features of a deforming armoured sidewall of a military vehicle submitted to an Improvised Explosive Device (IED) blast. A free moving impactor of 7 kg weight and 10 cm diameter contact face was propelled at 27 m/s and decelerated over 4 cm using copper tubes in order to control the penetration. Four tests on ES-2re 50th percentile dummy were performed to check on the similarity of the impact with an IED blast case. The Y shoulder force sensor time history signals were similar to ones recorded in full-scale IED blast tests. Six tests on Post Mortem Human Subjects were performed at different violence levels. The PMHS maximum deflections (from shoulder edge to sternum) and reaction force ranged from 3.2 cm to 4.7 cm, and from 5.7 kN to 11.7 kN, respectively. The three PMHS tests on which the highest forces were recorded presented moderate injury (AIS2) on the 2005 Abbreviated Injury Scale. Injuries were mainly humerus fractures (shaft and head). One subject sustained multiple fractures of the scapula. These results presented different features from those of previous studies that used lower impact rates (below 7 m/s). These results could be used to develop an AIS2+ shoulder injury criterion specific to these kinds of military impacts, using the ES-2re dummy.

Keywords improvised explosive device (IED), lateral impact, shoulder

I. INTRODUCTION

In the past fifteen years, protection of military vehicle occupants against landmines have become a major subject of concern for the Armies involved in asymmetric conflicts [1]. Particular attention has been paid to the blast Improvised Explosive Device (IED) threat [1]-[3] and research programs have been started within the past ten years among NATO countries to enhance the survivability of occupants of armored military vehicles exposed to such IED strikes [2].

Primary protection of the occupant is ensured by the integrity of the safety cell (occupant compartment), which strongly minimizes the effects of fragments, overpressure, gases and heat. However, even if the safety cell is not ruptured, the occupants can be injured via acceleration and blunt impacts. When it is sufficiently close, an IED blast first causes local deformation of the vehicle walls (primary phase), then a global acceleration of the entire vehicle occurs, and finally a possible resulting accident phase follows due to a lack of control of the vehicle [2].

Car crash dummies are commonly used in the military field to measure the body loads and estimate the risk sustained by the occupants. For the loadings caused by IED attacks, NATO experts made recommendations on the dummy model that should be used according to the attack scenarios and resulting loading directions [2]. For instance, the ES-2re 50th percentile male dummy was chosen for lateral loadings. Also, recommendations were made on the associated measurements and injury risk curves to be used to estimate the risk sustained by the occupants.

However, the NATO experts also pointed out limitations in the use of car crash dummies for the injury risk assessment. Among these, the shoulder force criterion associated with the ES-2re 50th percentile male dummy [2] was developed using PMHS data from the automotive field [2], and is, as far as IED blasts are concerned,

M. Lebarbé (email: mathieu.lebarbe@ceesar.asso.fr , tel: 01 76 87 35 19), J. Uriot, P. Potier and P. Baudrit are affiliated with CEESAR, European centre of studies on safety and risk analysis, Nanterre, France. D. LaFont is affiliated with DGA-TT, Division Générale de l'Armement – Techniques Terrestres, Bourges, France. G. Vallencien is affiliated with Université René Descartes, Paris, France.

applicable to blunt impacts resulting from the global acceleration of the vehicle but not to the high dynamic impacts resulting from the local deformation of the vehicle structure occurring in the primary phase of the explosion. For example, the wall submitted to an IED blast can deform at speeds rising up to 30 m/s but generally have limited intrusion on the occupant (~4 cm). Also, the impact duration is brief (~3 ms). These impact features differ significantly from the lower speed (3 to 10 m/s), longer duration (40-100 ms) impacts observed in the automotive field [10].

The scope of the present study was to provide new biomechanical data that could help the development of an ES-2re shoulder injury criterion valid at this high speed, short displacement lateral impact, which is typical in the military field. For this purpose, a test setup able to deliver this kind of impact was developed. Tests using ES-2re dummy were run in order to validate the test setup. Injurious and non-injurious tests on six Post Mortem Human Subjects (PMHS) were conducted in order to provide biomechanical data. A comparison of the PMHS responses with previous work on shoulder tolerance to lateral impact [7]-[12] was made.

II. MATERIAL AND METHODS

IED blast reference test

Specific test rigs have been developed by the German Army at the WTD91 (Wehrtechnische Dienststelle für Waffen und Munition) in order to perform full-size IED blasts with controlled and repeatable load transfer [1] [4-5]. For the lateral impact [5], it consisted in placing an ES-2re dummy in an armoured square cell, and performing an explosion close to the side wall of the cell (see Figure 13 in appendix). The armoured wall bulged out under the explosion, remaining in the elastic deformation domain, and retracted back. The dummy equipment and its distance from the side wall could be changed. During the tests, acceleration and displacement of the armoured wall were measured as well as the dummy shoulder force and ribs deflection. The reference test that the present study intended to mimic corresponded to an explosion of 30 kg of TNT located at 5 m from the cell. The distance between the dummy shoulder and the side wall was 10 cm. The wall deformed up to 14 cm. The maximum deformation speed was reached at 10 cm and was 27 m/s. Then, the deformation speed decreased quasi-linearly until it reached 14 cm deformation, where the wall retracted back (wall displacement and displacement velocity curves are shown in figure H-4 and Figure H-5 of [2]) .

Test setup

Figure 1 and Figure 2 give an overview of the test set-up with a subject in position prior to the test. A 7 kg circular impactor struck the shoulder of the surrogate laterally. Its head, made of aluminum, was a 100 mm diameter flat disc with 7 mm radius rounded edges. It was propelled at a velocity of 27 m/s using a pneumatic canon (see Figure 15 in appendix), and decelerated until 0 m/s over 4 cm using eight 82 mm long copper tubes acting on its tail. The subject was struck while the impactor was decelerated by the tubes. The impactor was in a free flight state prior to contact with either the copper tubes or the subject, and was guided during the impact.

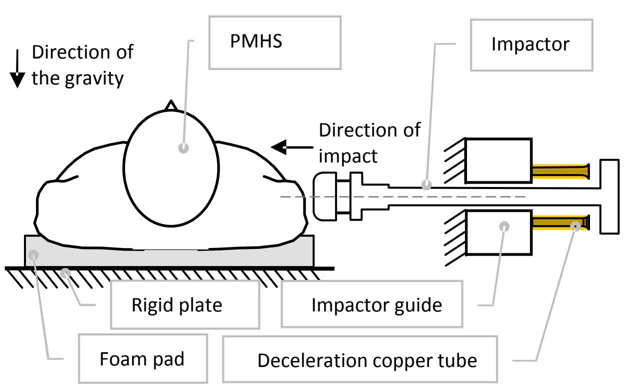

Figure 1: schematic front view of the test set-up.

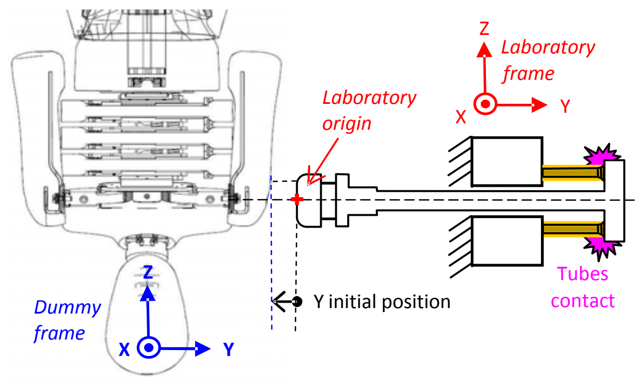

Figure 2: schematic top view of the test set-up.

The impactor main axis was aligned with the shoulder joint, i.e. the center of the humeral head for the PMHS and the center of the shoulder joint for the ES-2re dummy. The subjects were installed supine on a rigid plate to facilitate their positioning and the test repeatability. The rigid plate was adjustable along the three laboratory axes and maintained in position during the test using clamps. There was a chamber under it in order to place an X-ray cassette (36 x 43 cm) without perturbing the PMHS position.

Coordinate systems

ES-2re coordinate systems conformed to the SAE-J1733 standard. The PMHS global coordinate system was defined according to the dummy. The laboratory frame was orientated collinearly to the ES-2re frame, which was impacted at the right shoulder, i.e. the laboratory Y axis was defined by the impactor main axis and directed in the opposite direction of the impact (see Figure 1 and Figure 2). The origin of the laboratory coordinate system was defined at the center of the impactor circular interface when the tail of the impactor contacted the copper tubes (see Figure 2). This specific position of the impactor in the laboratory coordinate system will be called "the impactor neutral position".

Subject harvesting and preparation

ES-2re - The Eurosid-2re dummy (ES-2re) was calibrated prior to the tests. The dummy was mounted and equipped following the PADI revised in July 2004 (Procedures for Assembly, Disassembly and Inspection of the EuroSID-2re 50th Percentile Adult Male Side Impact Crash Test Dummy). The dummy was equipped with its jacket and the ribs were mounted for a right-side impact. The test room temperature was 20°C and the dummy rested several hours in it prior to the test.

PMHS – The Post Mortem Human Subjects (PMHS) were obtained through the center of the Body Donation to Science of the University René Descartes in Paris Vth after approval of the test protocol by the scientific and ethics committee. Among the PMHS available, the ones suspected of bone fragility (long bed stay, bone cancer, metastasis, etc) were excluded. Three PMHS were selected. Their features are given in Table 1. The PMHS were tested for Cytomegalovirus (CMV), Human T cell Leukemia/lymphoma Virus (HTLV), Hepatitis C Virus (HCV), Hepatitis B Virus (HBV) and Human Immunodeficiency Virus (HIV), and a medical survey was documented. Prior to the tests, subjects were injected with a broad spectrum of antibiotics in order to reduce the bacterial proliferation. Anthropometric details of the PMHS in a supine position on the autopsy table were measured with anthropometric calipers prior to testing. To further document anthropometric characteristics, CT scans of the complete body were also performed. These CT scans provided a 3D geometry of the skeleton. The specimens previously stored at -15°C were defrosted prior to instrumentation and dynamic test. At the time of the test, the body temperature was close to the ambient temperature (20° Celsius). The room temperature was maintained around 20°C up to the test. In order to maintain realistic pulmonary volumes, the PMHS lungs were inflated once, before the test, with approximately 2.5 liters of air through a tracheotomy tube that was held closed during the test.

Table 1 – PMHS features

PMHS n°	Age (years)	Gender	Weight (kg)	Stature [cm]	Shoulder breadth [cm]	Cause of death
643	68	Male	67	180	40,5	Lung cancer
644	67	Male	51	154,5	37,5	Bronchogenic cancer
645	75	Male	60	171	42	Cardiac arrest

Instrumentation

The impactor, PMHS and ES-2re were instrumented using the sensors listed in Table 2. All the sensors were glued on the bone component, except the T1 three axes accelerometer, which was firmly screwed on the vertebral body (see details in Figure 16 in the appendix). Both clavicle gages were located approximately at the junction between the proximal third and the median third of the clavicle. One gage was glued on the anterior part of the clavicle and the other one on the superior part. For the humerus, the sensors were located approximately at mid-distance between the head of the humerus and the elbow so that they could not be struck directly or indirectly by the impactor. All the measurements were acquired with a 100 kHz sampling rate data acquisition system. An anti-aliasing 20 kHz low-pass filter was applied on all the measurements.

Three high-speed cameras recorded the impact. The views are shown in Figure 3, Figure 4 and Figure 5. Cameras 1 and 2 filmed at a rate of 6000 images per second (6 kHz). They focused on the shoulder and the thorax to observe the body's response to the impact. The targets glued on the PMHS manubrium were tracked on the films of camera 2. Camera 3 filmed at a rate of 20 000 images per second (20 kHz). It zoomed on a small area to focus on the impactor head displacement. The film of camera 3 was used to backup the laser measurement of the impactor displacement. Targets were glued on the impactor head and on the impactor guide for that purpose (see Figure 4). The resolution was 1 mm/pixel for camera 2 and 0.5 mm/pixel for camera 3. The tracking was performed using Falcon™ software.

Table 2: overview of the instrumentation

	Location	Sensor	Sensor model
Impactor	Behind the head of the impactor.	3-axes load sensor	FTSS™ IF221
	Inside the head of the impactor.	Y axis accelerometer	Entran™ EGC-S042
	Between the impactor head and a fixed frame of the laboratory.	Y axis laser displacement sensor	Bullier™ M70LL
PMHS	Right clavicle, at the distal end of the first third.	2 strain gages along the longitudinal axis	Vishay Micro-Measurements™ CEA-13-125UN-350
	Left clavicle, at the distal end of the first third.	2 strain gages along the longitudinal axis	Vishay Micro-Measurements™ CEA-13-125UN-350
	Left ribs, arches n° 2 to 6, at the Median part, on the external side.	5 strain gages along the longitudinal axis (1 per rib).	Vishay Micro-Measurements™ CEA-13-125UN-350
	Right ribs, arches n° 2 to 6, at the Median part, on the external side.	5 strain gages along the longitudinal axis (1 per rib).	Vishay Micro-Measurements™ CEA-13-125UN-350
	Impacted humerus, at mid-diaphysis.	Y axis accelerometer 1 strain gage along the longitudinal axis	MEAS™ EGAS-S398A and MEAS™ 1201 Vishay Micro-Measurements™ CEA-13-125UN-350
	Sternum, on the manubrium.	3 accelerometers (along X, Y, and Z axes respectively)	MEAS™ EGAS-S398A
	T1 vertebra. On the vertebral body.	3 accelerometers (along X, Y, and Z axes respectively)	MEAS™ EGAS-S398A
ES-2re	Shoulder	3-axes load sensor Y axis accelerometer, glued on the load sensor	Standard sensor MEAS™ EGAS-S398A
	Ribs, impacted side.	Y deflection sensors Y axis accelerometers	Standard sensor Standard sensor

Figure 3 – Camera 1 view. Example with a PMHS.

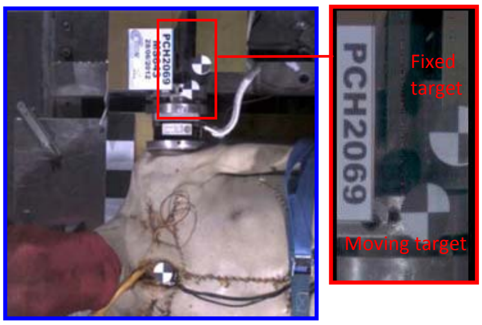

Figure 4 – Camera 2 (left) and camera 3 (right) views. Example with a PMHS.

Figure 5: Shot of camera 2. Example with a ES-2se dummy.

The impactor measurements (displacement, acceleration, force) were expressed in the laboratory frame. The PMHS and ES-2re measurements were expressed in their local body frames, which were not necessarily collinear with the laboratory frame. For instance, given the inclination of the humerus bone, a slight angle may exist between the Y axis of the accelerometer glued on the humerus dyaphysis and the Y axis of the laboratory frame. Moreover the local body frames, which are attached to body segments, move during the impact whereas the laboratory frame is steady.

Subjects' positioning procedure

The ES-2re dummy lay supine on the horizontal rigid plate with a Teflon low friction thin plate interface. The pivot stop plates of the arms held them in the 0° position. The symmetrical Y axis of the impactor was aligned with the center of the head of the screw linking the arm to the thorax (part n°5000040). X and Z coordinates of the shoulder screws were set to 0 using a 3D articulated arm. The hips and the knees were 90° flexed, the feet lying on a tablet.

For the PMHS, a soft foam pad (52x62x5 cm) was placed between the back of the subject and the rigid plate to minimize a potential constraint of the scapula by the plate. Attention was paid to get a physiologic straightness of the spine in YZ plane (frontal plane) while placing the flaccid specimen on the back. The head was supported by a P.V.C. headrest "6 positions". A slight flexion was applied to the neck in order to avoid interaction of the back bottom of the head with the accelerometer plate installed on T1 vertebra. The arms rested along the torso and the thigh lay on a tablet. The knees were 90° flexed and the feet stood on the ground.

The arms were in adducted position along the long axis of the body (at side). The wrists were turned in external rotation, contributing to the adduction of the upper arm. Then, the arms were pulled toward the feet (in the local Z direction) in order to have a position of the shoulder girdle similar as when the torso was upright. The arm was held in that position by tightening a strap around the wrist.

The rigid plate was moved in the horizontal plane in order to have the PMHS global frame collinear with the laboratory frame as suggested in Figure 1 and Figure 2. The symmetrical Y axis of the impactor was aligned with the center of the humeral head, which was considered as a sphere (Figure 6). This positioning was reached using two X-rays taken at different angles (Figure 6).

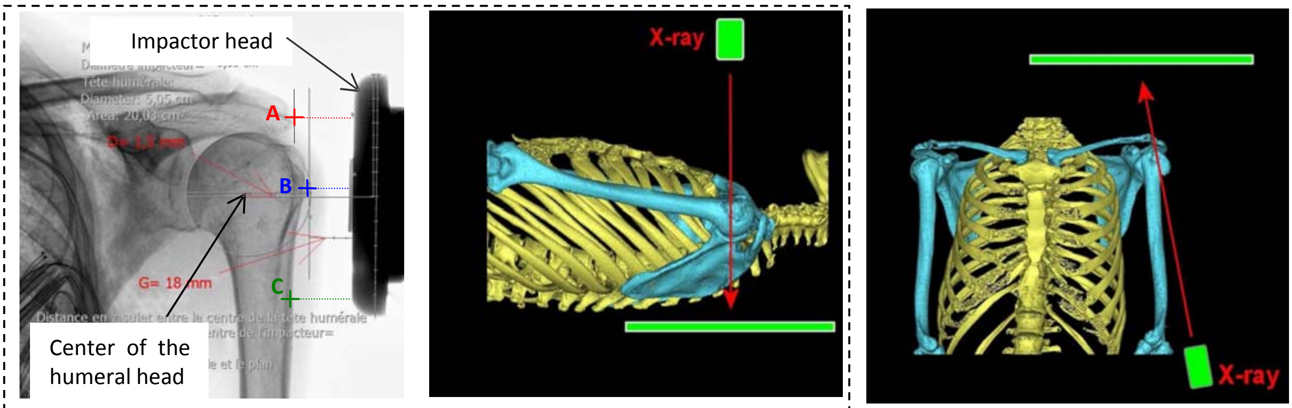

Figure 6 – Right and center: Directions of the central ray for the two X-rays used to align the center of the humeral head with the impactor. Left: Result of the face view X-ray. A: lateral edge of the acromion; B: external lateral edge of the humeral head; C: lowest point on the external side of the humerus diaphysis, at the beginning of the impactor round edge.

Y Initial position

Once the shoulder joint was properly aligned with impactor, the Y initial position of the subject in the laboratory coordinate system was adjusted. As illustrated in Figure 2, it corresponded to the Y coordinates of the first component of flesh or jacket touched by the impactor. Note that for the ES-2re dummy, and for some PMHS, the shoulder extremity was below the impactor symmetric axis because of the inclination of the arm.

The Y initial position of the subjects was varied from one test to another in order to vary the violence of impact.

Measurement of the subject initial position

Just prior to the test, a 3D measuring arm (Romer™ type 100) was used to record the initial position of targets and landmarks of the subject in the laboratory coordinate system, such as bone tuberosities for the PMHS or hard structure components for the ES-2re. Also, the face view X-rays taken just before the test were used to have an estimate of the position of some shoulder bone components with respect to the impactor when it contacted the shoulder skin (see Figure 6). The X-ray measurement plane (YZ plane passing by the impactor head center) was calibrated using a 30 mm long radio-opaque marker installed at the center of the impactor along the Z axis. The digitizing AGFA NX software was used to measure the distances. The X-ray filter was set to optimize the definition of the bone contours.

Injury assessment

One face view X-ray of the shoulder was taken just after the test, the body untouched on the test rig. Then an in-depth biomechanical autopsy of the shoulder was performed. The details of the anatomical parts that were dissected and assessed are given in Table 3. Pictures of the injured organs were taken.

Table 3 – PMHS anatomical parts that were examined during the necropsy

- Integuments of the shoulder, thorax and arm
- Muscles of the scapular belt, thorax and arm
- Ligaments and capsule: sternoclavicular joint and ligaments, acromioclavicular joint and ligaments, glenohumeral joint and ligaments, conoid ligament, trapezoid ligament, acromioclavicular ligament.
- Bones of the scapular belt, thorax and arm: humerus, scapula, clavicle, ribs, sternum
- Arteries: brachiocephalic trunck (right), common carotid artery, subclavian artery, axillary artery, brachial artery, suprascapular artery.
- Veins: brachiocephalic vein, subclavian veins, axillary vein, surpascapular vein, cephalic vein, brachial vein.
- Nerves: brachial plexus, median nerve, radial nerve, ulnar nerve, musculocutaneous nerve, superior subscapular nerve, suprascapular nerve, long thoracic nerve.
- Thoracic inner organs: lungs, pleura, mediastinum.

Bone mineralization

In order to have an estimate of the bone strength, the mineral density (C/V in g/cm^3) and the mineral linear density (C/L in g/cm) of the medium part of the 4th ribs were measured according to the method reported by Charpail et al. [6].

Data processing

The offsets of the acceleration, load and strain measurements were removed by subtraction of the mean value calculated in a 490ms-window before the triggering of the piston propelling the impactor. The load sensor was polarized so that it expressed the force applied by the tail of the impactor against the impacting face. For the PMHS impacted on the left side, the sign of the measurements along the Y axis was reversed in order to be easily compared with the right-impacted PMHS. For the strain gages, a positive signal indicated tension.

The filters that were applied for each measurement are given in Table 4. The ES-2re dummy measurements were filtered according to the SAE-J211 standard. The PMHS accelerations were filtered at CFC (Channel Frequency Class) 2000 and the strain signals were let unfiltered.

Table 4: post processing of the measurements

	Location	Measurement	Filter
Impactor	Load sensor - force applied by the tail of the impactor against the impacting face	Y force	CFC 2000 or 1000
	Inside the head of the impactor.	Y acceleration	CFC 2000 or 1000
	Between the impactor head and a fixed frame of the laboratory.	Y displacement	CFC 600
PMHS	Right clavicle, at the distal end of the first third.	Strains along the longitudinal axis.	Unfiltered
	Left clavicle, at the distal end of the first third.	Strains along the longitudinal axis.	Unfiltered
	Left ribs, arches n° 2 to 6, at the Median part, on the external side.	Strains along the longitudinal axis.	Unfiltered
	Right ribs, arches n° 2 to 6, at the Median part, on the external side.	Strains along the longitudinal axis.	Unfiltered
	Impacted humerus, at mid-diaphysis.	Y acceleration Strain along the longitudinal axis	CFC 2000 Unfiltered
	Sternum, on the manubrium.	Y acceleration	CFC 2000
	T1 vertebra. On the vertebral body.	Y acceleration	CFC 2000
ES-2re	Shoulder	Y force	CFC 600
	Ribs, impacted side.	Y deflections	CFC 180

For the impactor acceleration and force, two levels of filtering were used. The CFC 1000 filter was applied to display the curves and to extract the peak values. This filter class was necessary to really clean the signals from the oscillation artifacts induced by the deceleration against the tubes. However, impactor force and acceleration measurements were also used to determine the time of impact. In that case, the CFC 2000 filter was used for it allowed removing the major oscillation artifacts without too much smoothing and stretching of the curve toe before the rise from 0. The impactor displacement was filtered at CFC 600.

The subject's reaction force was computed using Newton's second law, applied to the impactor head, considered as a rigid part (see Equation 1). The force applied by the copper tubes on the impactor was computed following Equation 2. The mass of the impactor head, which included necessarily a part of the sensor mass, was determined during the impactor propelling phase, when only the load sensor acted on the impactor head (**$F_{shoulder\ /\ impactor\ head}=0$**). The impactor head mass ($m_{impactor\ head}$) was found to be 0.46 kg. The total impactor mass ($m_{impactor}$) was 7 kg.

Equation 1: $F_{shoulder/impactor\ head} = m_{impactor\ head} * \gamma_{impactor\ head} - F_{load\ sensor}$

Equation 2: $F_{tubes/impactor\ tail} = m_{impactor} * \gamma_{impactor\ head} - F_{shoulder/impactor\ head}$

The time of impact (T_I) was identified by the rise of the subject reaction force curve computed using CFC 2000 filtered load cell and acceleration signals. The subject reaction force curve was screened from the right to the left (inversely from the time flow), starting from a significantly high value (maximum peak for instance) until reaching a threshold of 300 N, which was considered as the time of impact. The impactor penetration was defined as the impactor displacement, starting from the time of impact (T_I). The shoulder total deflection was computed by subtracting the sternum displacement from the impactor displacement, starting from the time of impact (T_I). The impactor velocity was computed by integration of the CFC 1000 filtered acceleration signal.

Test Matrix

Four tests on 50th percentile ES-2re and six tests on three PMHS (one impact per shoulder) were performed. The test matrix is shown in Table 5.

A Y initial position of 0 cm corresponded to a shoulder-wall gap of 10 cm in the full-scale test [5].

For each PMHS, it was attempted to do one non-injurious test (less than AIS2) on one shoulder, and one injurious test on the opposite shoulder (AIS2+).

Table 5 – Test matrix

Subject	Test n°	Impacted side	Targeted Y Initial position (mm)
ES-2re	PCH2060	Right	0
	PCH2061	Right	0
	PCH2062	Right	10
	PCH2063	Right	10
PMHS 643	PCH2069	Left	-10
	PCH2070	Right	3
PMHS 644	PCH2071	Left	-5
	PCH2072	Right	0
PMHS 645	PCH2073	Left	10
	PCH2074	Right	0

III. RESULTS

Impactor decelerations

Figure 7 shows the impactor deceleration time history for all the 10 tests. The time 0 corresponded to the time of tubes contact. The oscillations of the signal were due to the deformation of the copper tubes. The copper tubes induced a deceleration with a global trapezoidal shape. The mean deceleration of the plateau was between 9500 and 1000 G's. For the tests with a positive Y initial position, the shoulder was impacted slightly before the copper tubes acted, and the impactor deceleration started earlier than time 0.

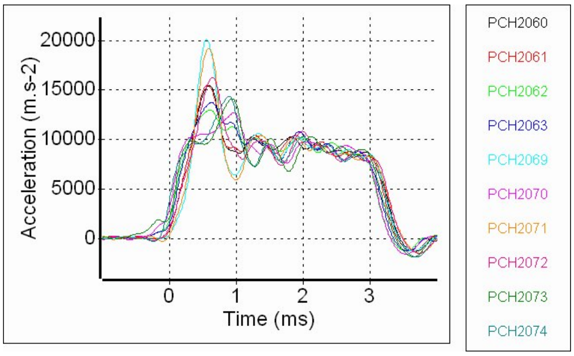

Figure 7 – Impactor deceleration time history (CFC 1000). Time 0 is the time of tube contact.

ES-2re dummy results

The whole body Y reaction force and the load recorded in the shoulder sensor Y axis are shown in Table 10 for all the dummy tests. The test repeatability was satisfactory. The duration of the impact was ~3.5 ms and the body reaction forces rose up to 6.8 kN and 8.8 kN for the 0 and 10 mm Y initial position, respectively. The load in the shoulder started at 0.6 ms and lasted until 7.5 ms approximately for all the tests, and peaked at -2.4 kN and -2.9 kN for the 0 and 10 mm Y initial position, respectively. The maximum ribs deflection was recorded on the upper rib, and was -5 mm @ 13 ms and -8.5 mm @ 12 ms for the 0 and 10 mm Y initial position, respectively. For all the tests, at the end of the impact (3.5 ms), the ribs did not demonstrate significant deflection and the sternum did not move. The lower and middle ribs peak deflection was less than -2 mm at 23 ms and 16 ms, respectively.

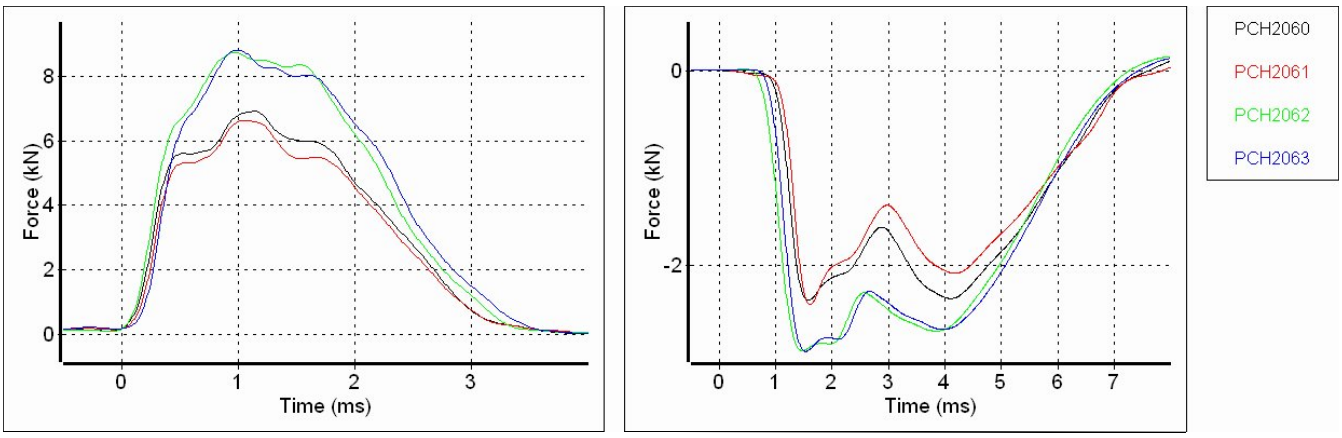

Figure 8 – For the four ES-2re dummy tests. Left graph: Whole body Y reaction force time histories. Right graph: Y shoulder force time histories

PMHS results

Injuries – The injury details and the corresponding AIS score are given in Table 6. Post test x-rays and pictures of the bone fractures are shown in the appendix in Figure 31 to Figure 33 and in Figure 17 to Figure 30 respectively. Three tests induced AIS1 injuries and the three others AIS2 injuries. All the tests presented a crush injury of the integument and the deltoid muscle facing the center of the impactor. The three AIS2 tests all presented fractures of the humerus diaphysis. Both PMHS 644 shoulders did not sustain more than AIS1 injury (PCH2071, PCH2072). Both PMHS 645 shoulders sustained AIS2 injuries (PCH2073, PCH2074) but differences in the amount of injuries could be seen. As the MAIS score of the shoulders were either 1 or 2 for the six tests, an additional injury scale was added in Table 6 to better reflect the severity of the damage sustained by the shoulders. This is the "TAIS", i.e. the total of the AIS scores of all the injuries found in the shoulder segment.

Table 6 – Injury results from autopsy and bone mineralization

PMHS n° *c/L (g/cm)* c/V (g/cm^3)	Test n° Imp. side	MAIS* *TAIS***	Injury details
643 *0.245* 0.285	PCH2069 left side	1 *1*	· Soft tissues: Crush injury of the integument and the deltoid muscle facing the center of the impactor (AIS98: 1, AIS2005:1).
	PCH2070 right side	2 *5*	· Soft tissues: o Crush injury of the integument and the deltoid muscle facing the center of the impactor (AIS98: 1, AIS2005:1). o Crush injury of the capsule without rupture (AIS98: 0, AIS 2005: 1) · Joints: o Acromioclavicular joint sprain grade I according to the Rockwood classification (AIS98: 1, AIS2005: 1) · Fractures: o Non comminuted diaphyseal fracture below the surgical neck and facing the impactor (AIS98: 2, AIS2005: 2) o Crush 5 mm deep of the lateral edge of the acromion (AIS98: 0, AIS 2005: 0)
644 *0.26* 0.49	PCH2071 left side	1 *1*	· Soft tissues: Crush injury of the integument and the deltoid muscle facing the center of the impactor (AIS98: 1, AIS2005:1).
	PCH2072 right side	1 *1*	· Soft tissues: Crush injury of the integument and the deltoid muscle facing the center of the impactor (AIS98: 1, AIS2005:1).
645 *0.16* 0.315	PCH2073 left side	2 *13*	· Soft tissues: Crush injury of the integument and the deltoid muscle facing the center of the impactor (AIS98: 1, AIS2005:1). · Humerus fractures: o Comminuted diaphyseal fracture facing the impactor (AIS98: 3, AIS2005: 2). o Comminuted fracture of the humeral head involving the cartilage (AIS98: 3, AIS2005: 2). o Fracture of the anatomical neck (AIS98: 2, AIS2005: 2). · Scapula fractures: o Acromion fracture without displacement (AIS98: 2, AIS2005: 2). o Fracture with displacement of the coracoid process at the level of its base (AIS98: 2, AIS2005: 2) o Incomplete fracture of the supraspinatus fossa (AIS98: 2, AIS2005: 2).
	PCH2074 right side	2 *8*	· Soft tissues: o Crush injury of the integument and the deltoid muscle facing the center of the impactor (AIS98: 1, AIS2005:1). · Joints: o Complete disruption of the capsule from the anterior insertion to the posterior insertion involving the associated ligaments (AIS98: 2, AIS2005: 1). · Fractures : o Comminuted diaphyseal fracture facing the impactor (AIS98: 3, AIS2005: 2) o Fracture of the anatomical neck (AIS98: 2, AIS2005: 2) o Comminuted fracture of the humeral head without involvement of cartilage (AIS98: 3, AIS2005: 2)

* MAIS is the maximum of the AIS 2005 scores for each test
** TAIS is the sum of the AIS 2005 scores for each test.

Bone mineralization – The bone mineralization values of the three PMHS are given in Table 7 and recalled in Table 6. The average and standard deviation of the C/L and C/V values of a total of sixty eight PMHS tested in CEESAR facilities are given in Table 8. The mineralization values of the PMHS tested in the present study were in the range of the common values, except for the PMHS 644, which C/V value (0.49 g/cm^3) was above the standard deviation higher bound (0.46 g/cm^3).

Table 7 - C/L and C/V values of the three PMHS tested in the present study

PMHS N°	643	644	645
C/L (g/cm)	0.245	0.26	0.16
C/V (g/cm^3)	0.285	0.49	0.315

Table 8 - Average and standard deviation of the C/L and C/V values of sixty eight PMHS tested in CEESAR facilities

	Average	SD
C/L (g/cm)	0.23	0.08
C/V (g/cm^3)	0.36	0.1

Impact penetration and force response – The PMHS measurement time histories are shown in Figure 9 and the main characteristics of the impacts are summarized in Table 9. All the PMHS were impacted approximately at the same speed (~27 m/s). The body reaction force peaked early after shoulder contact, between 0.31 ms and 0.71 ms, which correspond to 8 to 17 mm impactor penetration. The end of the impact was defined at the time of maximum impactor penetration. At this time, no load was applied on the shoulder anymore. The duration of the impact was 2.3 to 2.8 ms The impactor maximum penetrations ranged between -32 and -50 mm and occurred after the end of the load. The sternum displacements began late during the impact and did not exceed 3 mm at the end of the impact. Therefore, the deflection maximum values were very close to the penetration maximum values for all the tests. The body reaction force could be sorted into two groups of similar magnitude and shape. It appeared that the group with the higher forces corresponded to the most injured PMHS (AIS2).

Accelerations – From Figure 9, we observed that the sternum, spine and humerus Y accelerations peaked after the body reaction force. The humerus Y acceleration signal started almost simultaneously with the force signals. Sternum and spine Y accelerations began to rise around 1 ms after the impact. The humerus Y accelerations peaked higher than the two others. The sternum Y accelerations peaked approximately twice higher than the T1 vertebra Y accelerations.

Table 9 – Main characteristics of the impacts on the PMHS.

	Y initial position (mm)	Impact speed (m/s)	Max. reaction force (kN)	@ time (ms)	Pene at max reaction force (mm)	Max. pene. (mm)	@ time (ms)	Max. def. (mm)	@ time (ms)
PCH2069	-8	-26.6	6.6	0.67	-15	-32	2.8	-31	2.7
PCH2070	6	-27.4	10.3	0.36	-10	-43	3.2	-42	3.1
PCH2071	-4	-27.3	5.8	0.71	-16	-35	2.9	-35	2.8
PCH2072	1	-27.7	7.0	0.52	-14	-40	3.0	-40	2.9
PCH2073	13	-27.5	11.5	0.60	-15	-50	3.4	-48	3.3
PCH2074	1	-27.4	10.4	0.31	-8	-40	3.1	-38	2.8

Strains, impacted side – All the strain signals peaked after the force, except the humerus strains of PCH2073 and PCH2074. The humerus strain signals were detected almost immediately after the impact, followed by the ribs strain signals and then the clavicle strain signals. Humerus strain gages exhibited compression, clavicle strain gages exhibited compression, ribs strain gages exhibited tension or compression according to the test.

Strains, opposite side – The opposite clavicle and ribs demonstrated very flat strain signals, which started rising around 1.8 ms approximately.

Shoulder bone landmark distances from the impactor – Table 10 gives the distances of the lateral edges of some shoulder bone components from the impactor in contact with the shoulder edge along the Y laboratory axis. The sternum and the acromioclavicular joint landmark distances were extracted from the 3D arm records. The others were measured on the pre-test X-rays.

Table 10 – Y distances of shoulder bone landmarks from the impactor at skin contact. They were measured on X-rays, except the acromio-clavicular joint and the sternum that were extracted from the 3D arm records. The distances are given in mm.

PMHS n°	Test n°	Humeral head	Acromion	Humerus shaft point	Acromio clavicular joint*	Sternum**
643-L	PCH2069	-13	-20	-24	-44	-224
643-R	PCH2070	-17	-26	-26	-56	-230
644-L	PCH2071	-20	-31	-29	-55	-214
644-R	PCH2072	-25	-37	-30	-68	-218
645-L	PCH2073	-18	-23	-24	-45	-228
645-R	PCH2074	-15	-25	-24	-48	-232
Mean		**-17.9**	**-27.0**	**-26.2**	**-52.7**	**-224.4**
SD		4.3	6.1	2.7	9.1	7.3

* this landmark was palpated through the skin. The precision is ± 10 mm.

** center of the accelerometer, which was glued at the center of the manubrium

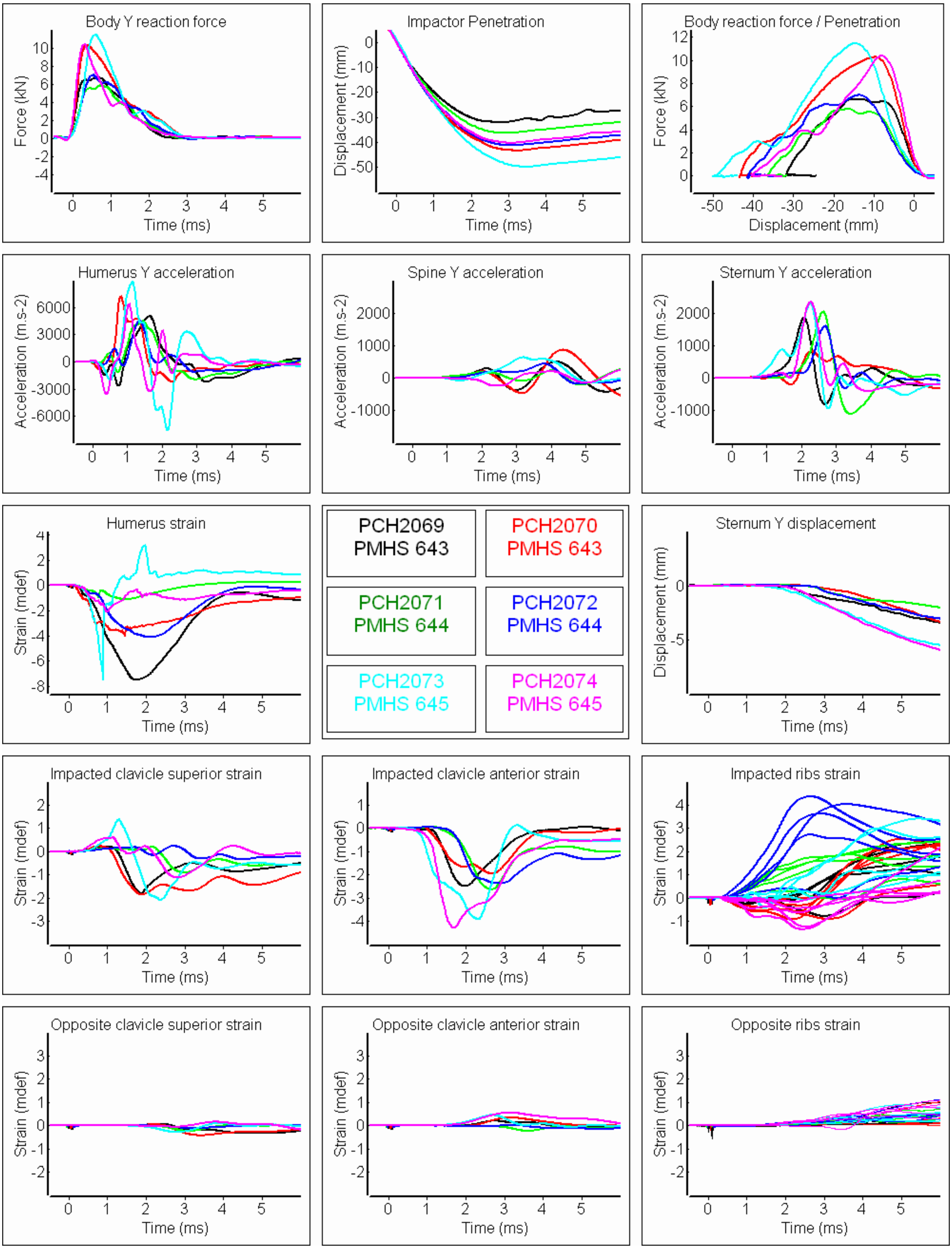

Figure 9 – Time histories of the measurements recorded on the six PMHS tests. The penetration of the tests PCH2071 and PCH2073 were tracked on the movies of camera 3 because the laser displacement sensor failed. The body reaction force as a function of the impactor penetration is shown on the upper right graph.

High speed movie observation – For each test, the following could be observed on the movies: the impactor seemed to stamp into the shoulder without any other motion of the body but a wave that propagates through the surrounding soft tissues of the shoulder. Significant motion of the body could not be seen before approximately 5 ms. Images extracted from the movie of test PCH2073 are shown as an example in Figure 10.

Contact Ti	Fmax Ti + 0.6 ms	Ti + 1.5 ms	Dmax Ti + 3.5 ms	Ti + 5 ms

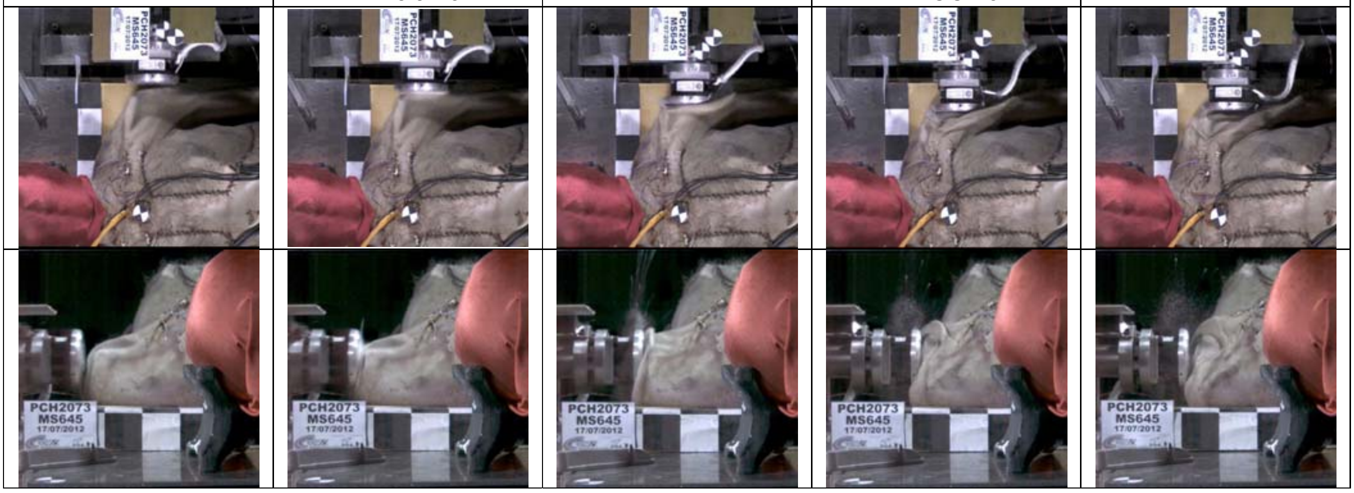

Figure 10 – Images from the movies of test PCH2073 during and after the impact.

IV. DISCUSSION

Subject supine position

Dimensional constraints of the test set-up lead to installing the subjects supine for being impacted. However, several measures were taken to get the thorax and the shoulder girdle posture close to a seated position. Firstly, the foam under the back of the PMHS had to prevent an exaggerated backward initial position of the shoulder joint. Secondly, attention was paid to get a physiologic straightness of the spine in the YZ plane (frontal plane) while placing the flaccid specimen on the back. In addition, the arms were pulled toward the feet (in the local Z direction) in order to have a position of the shoulder girdle similar to when the torso was upright.

Moreover, it is believed that this supine test procedure had some advantages compared to the seated one: 1) it facilitated the initial positioning of the subjects. 2) Bolte et al. [7] mentioned that the "hunch" of the shoulder of the PMHS was not controlled when positioning the subject. The supine position on the foam pad would favor a more repeatable shoulder posture.

Representativeness of an armoured wall deformation induced by an IED blast

Figure 11 compares the ES-2re Y shoulder forces obtained with the tests of the present study on the one hand and with two full-scale tests of the WTD91 [5] on the other hand (given in Figure 14 in appendix). The curves from the full-scale tests were switched to the left to have the time of impact correspond. It can be observed that the force responses were very close in intensity and duration, and the shapes were similar. Therefore, the test set-up of the present study was considered as valid to mimic the loading of a deforming armoured wall blasted by an IED. However, one limitation should be underlined that the impactor contact surface was only a 10 cm diameter disc compared to a whole wall for the WT91 full-size test, which may induce differences in the loading and the PMHS injury outcome. Differences were noticed on the ES-2re ribs maximum deflection. For the full-size tests, the middle rib deflected up to 15 mm maximum, and for the present tests, the upper rib deflected up to 5 cm maximum. This underlines a different involvement of the arm on the thorax loading. Beyond the difference in the loading surfaces, it may be due to the maximum deformation of the plate of the full scale tests, which could have occurred at the level of the middle rib and not at the level of the shoulder.

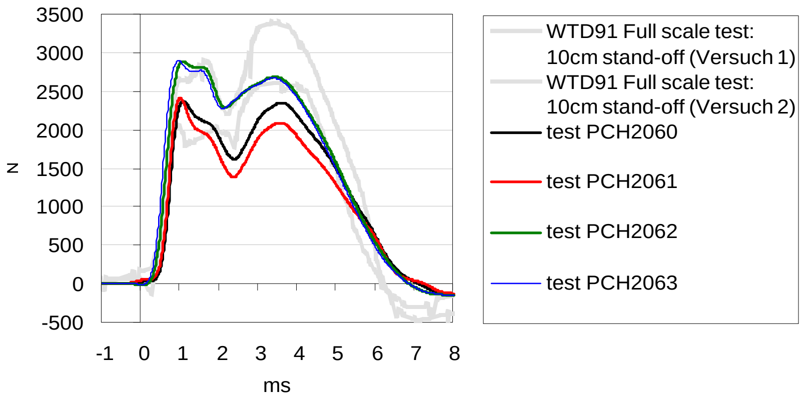

Figure 11 – Comparison of the ES-2re Y shoulder force responses (cfc 600 filtered)

Table 11 – Comparison of the ribs maximum deflection between CEESAR and WTD 91 tests

Labo.	Test n°	Dmax (mm)	Rib level
WTD 91	Versuch 1	15	Middle
	Versuch 2	15	Middle
CEESAR	PCH2060	5	Upper
	PCH2061	4	Upper
	PCH2062	8	Upper
	PCH2063	8	Upper

PMHS shoulder reaction to a high speed – short displacement impact

General behavior – The results provide several evidences of a localized reaction of the shoulder during the impact, as suggested by the movies.

The maximum force occurring early during the impact and the propagation wave of surrounding flesh observed in the movie suggests that the intensity of the force would be due primarily to the mass and the viscosity of the tissue localized just under the impactor face. Then the force dropped down rather quickly under the action of the copper tubes.

The observation of the PMHS measurement time histories in Figure 9 allows drawing a rough chronology of the PMHS response. According to the acceleration and strain signals, the humerus bone reacted rather quickly after the impact, followed by the rib cage, then by the clavicle (impacted side), and finally by the sternum and the T1 vertebra. The acceleration at the sternum was twice higher than that at the T1 vertebra. This was likely due to a transmission of the load to the sternum through the clavicle in addition to the ribcage path.

However, the low strain signals at the opposite of the body (clavicle and ribs), which occurred late during the impact, and the minimal motion of the sternum at the end of the impact occurring late support little involvement of the opposite half body. Furthermore, no clavicle or rib fractures were observed for all the tests, suggesting an even more localized involvement of the shoulder.

The autopsies revealed crush injuries of the integument and the deltoid muscle facing the center of the impactor for all the tests. This observation suggests that the tissues were highly compressed against the humeral head. Also, for the three PMHS which sustained bone fractures, the humeral diaphysis was fractured each time at the level of the impactor edge (see Figure 31 to Figure 33). Moreover the humeral head fractured or totally collapsed for the tests PCH2074 and PCH2073. Again, these results suggest that the motion of the impactor was so high that it stamped the humerus, inducing a shear of the diaphysis and a squeeze of the humeral head without giving time to the other bone components (scapula, clavicle) to move.

Injury result explanatory parameters – Various criteria commonly assessed as injury explanatory parameters were considered and cross-plotted with the total AIS score (TAIS 2005, see Table 6):

- the total deflection (max. deflection in Table 9)
- the total compression: total deflection divided by the [Sternum-Shoulder contact] distance in Table 10
- the "skeletal deflection": total deflection minus the [Humeral head-Shoulder contact] distance in Table 10
- the "skeletal compression": "skeletal deflection" divided by the [Sternum-Humeral head] distance in Table 10
- the "skeletal penetration": max impactor penetration (Table 9) minus the [Humeral head-Shoulder contact] distance in Table 10)
- the maximum body reaction force (in Table 9)

The considered criteria are given in Table 14 in the appendix and the cross-plots are shown in Figure 12 (graphs "a" to "f"). The graph "a" suggests that the total deflection is not fully satisfactory as an injury explanatory variable. The graph "b" shows that the injury prediction could not be enhanced by using the total compression instead of the total deflection. The graphs "c" and "d" suggest that the uses of the "skeletal deflection" (an indicator of the humeral deflection) or the "skeletal compression" would allow enhancing the injury prediction. The graphs "c" and "e" show that using the skeletal penetration instead of the skeletal deflection does not modify the quality of the correlation with the injuries. The graph "f" shows that the body reaction force could be a good injury predictor in the present test conditions.

The seriousness of the injuries seemed to be better related with the impactor penetration into the skeleton. This would explain why the test PCH2072, expected to be injurious compared to the test PCH2071 conducted on the same PMHS, was not. Indeed, for the test PCH2072, the shoulder edge initial position was closer to the impactor neutral position than the test PCH2071, but the humeral head and the acromion were further away, yielding identical skeletal penetration (-16 mm). In addition, this PMHS may have had stronger bones than the two others of the series. Indeed, the C/V mineralization value was the highest of the three PMHS and was above the standard deviation computed on 68 PMHS.

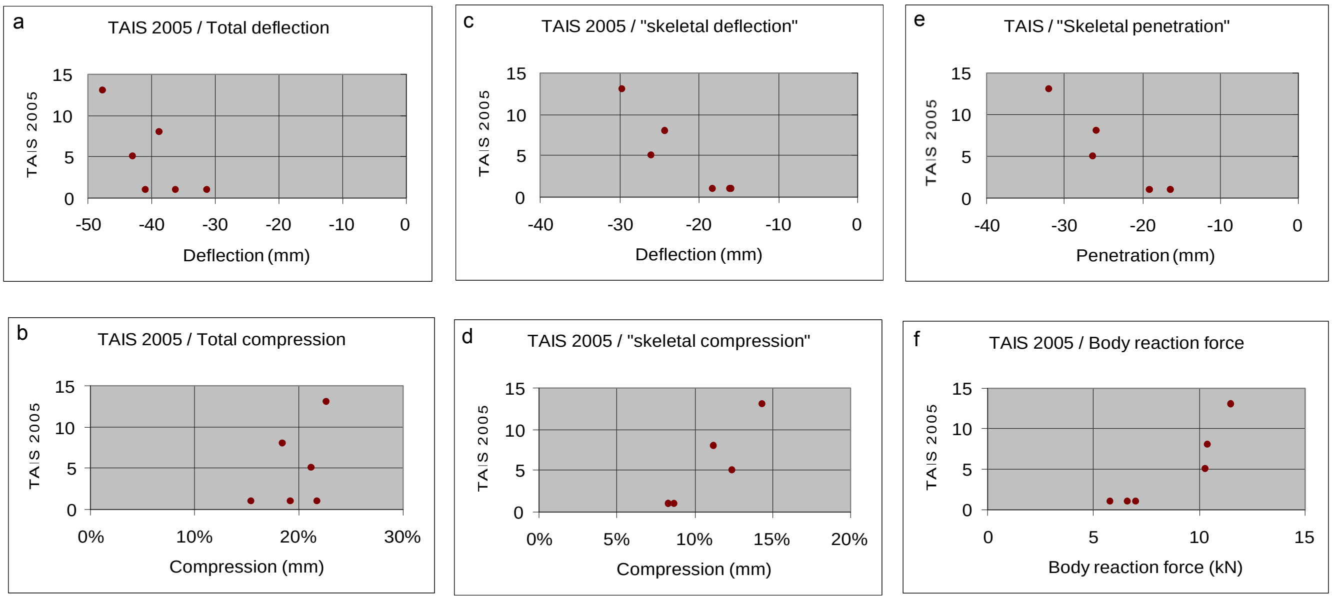

Figure 12 – Injury result as a function of various criteria

Comparison with the previous shoulder impact studies

Force response – It was observed that the force levels differed between the present study and previous automobile-like impact studies. For the present study, the peak values ranged from 6 kN to 11 kN and occurred very soon after impact, whereas for the previous impactor studies ([7-9, 12]) the peak forces ranged generally from 2 kN to 4.5 kN and occurred later. This may be due primarily to the differences in impact speed (27 m/s versus 3-10 m/s respectively).

Indeed, for the present study the impactor force reached a peak early which quickly diminished under the deceleration of the tubes. The penetration into the body was also limited. As a result, a small mass portion of the body was involved, suggesting that the impact speed prevailed in the body reaction force result. For the previous studies, a free flight 23.4 kg mass impacted the subjects at a determined speed and most of the energy was transferred to the body. Force/deflection curves showed that the body reaction force first sharply rose under the inertia and viscosity of the soft tissues, and continued gently to increase by recruiting more body mass, in particular through the shoulder bones. In that case, the peak force levels were due to both the impact speed and the recruited effective mass. However, the observation of the force/deflection curves also demonstrated that at least half of the reaction force was reached at the beginning of the impact, making the impact speed a significant parameter.

Injury features and mechanism – In the previous laboratory and automobile field studies [7]-[12], the distal clavicle fracture was the most frequently reported AIS2 injury, whereas it was the humerus fracture for the present study. However, for the rigid impacts [9]-[12] acromion and coracoid process were also frequently reported and one test of the present study also induced these injuries (PCH2073). This was the test for which the penetration was the most important (see Table 9).

Despite a similarity with the acromion fracture, the injury mechanism seems to differ between automobile and military impacts. Slower impact motion would allow pushing the humerus without breaking it. As suggested by Koh et al. [12], this would allow a global deformation of the shoulder girdle and would result in joint failure by tearing of the ligaments, inducing distal clavicle fractures. The rib fractures that occurred sometimes [9, 12] would also be a result of this lateral motion of the humerus penetrating into the thorax. On the contrary, high speed-short penetration impacts would crush the shoulder without allowing any global motion during the impact. This would induce mainly humerus fractures.

The PMHS which sustained the highest impactor penetration (PCH2073) presented acromion, coracoid process and scapula fractures. Koh et al. [10] and Compigne et al. [9] established that the acromion was more likely to fracture when the impactor was unpadded. Considering the rigid impact cases, the authors also underlined that the acromion injury appearance depended on the location of the impact on the shoulder. The acromion was less exposed if the humeral head was loaded first. In the sled test described in Koh et al. [10], the hand palms were lying on the lap. It was hypothesized that the induced posture of the arm and shoulder joint contributed to expose the acromion before the humeral head. In the present study, the gap between the lateral humeral head tuberosity and the lateral edge of the acromion was maximized by rotating the arm outward around the Z axis. Thus, the humeral head was clearly impacted first. The acromion/scapula fracture observed for the test PCH2073 of the present study would be due to a direct contact of the impactor on the acromion, after the collapsing of the humeral head.

Injury criteria – The comparison with previous research should be made cautiously because the injury nature in the present study (mostly humerus failure) was found to differ with the one of previous studies (mostly clavicle fractures).

The peak reaction force was not found to be a good injury predictor in the previous studies [9, 12]. Despite the fact that only six tests were performed, the result of the present study suggested the opposite. But part of the load was absorbed by a deceleration system whereas it was not for the previous study. Consequently, as far as injury criterion is concerned, the peak reaction forces of the present study should not be compared to the ones of the previous low speed impact study. However, if it is confirmed that the force is a good injury explanatory parameter to consider for military-type impacts, it may be interesting to associate it with another parameter such as the impact speed, the impact duration or the impactor penetration to take into account the specifics of each loading and develop an injury criterion applicable to all kinds of shoulder lateral impacts.

The skeletal deflection was found to be a good injury predictor in the previous and present studies. Koh et al. [12] synthesized the data of all previous impactor studies [7-9, 11] and proposed an injury criterion based on the acromion-to-T1 2D deflection. To compare with the previous studies, an estimator of the 1D acromion deflection was computed (see procedure in Table 12 and results in Table 14 in appendix). Given the fact that the sternum virtually does not move till the end of the impact, and that the T1 vertebra accelerations were much lower than the sternum ones, it was hypothesized that this acromion deflection estimator could be compared to acromion-to-T1 2D deflection measurements reported by Koh et al. [12]. However, Compigne et al. [9] observed that 2D deflection values were higher than 3D values. This was likely due to a forward movement of the acromion or a global rotation of the body around the Z axis. For similar reasons, it may happen than these 2D deflection values were lower than the 1D deflection that would have been measured along the Y axis. In addition, in the automobile impactor tests, differences were observed between acromion-to-T1 and acromion-to-sternum peak values. The comparison should be made cautiously.

Table 12 - Rationale and computation of the acromion deflection estimator

- The acromion deflection estimator was computed by subtracting the distance between the shoulder edge contact point and the acromion edge to the total deflection. Additional 3 mm of supposed compressed soft tissue were subtracted.
- An error bar of ± 3 mm was added to get lower and higher bounds:
  - in the higher bound case, it was hypothesized that the impactor was completely in contact with the acromion, the flesh would have totally vanished or would have been crushed to a negligible thickness, and that the acromion would not move from its pre-test initial position until impactor contact.
  - in the lower bound case, it was hypothesized that a higher quantity of flesh remained between the impactor and the acromion, for instance due to a higher thickness and a lower compressibility of the dermis and epidermis, and that the acromion started to move laterally before the impactor reached the point of its initial position.

The lowest deflection values at which an AIS2 injury was observed are presented in Table 13. They ranged between 31 mm and 39 mm. Five tests sustained a distal clavicle fracture and the sixth test sustained scapula fracture, including acromion fracture. In the present study, the maximum reached by the 1D deflection estimator was 27 mm (see Table 14 in appendix) and was associated with humerus and scapula fractures (PCH2073). The lack of clavicle fractures in the present study may be explained by too short a penetration of the impactor. However, humerus fracture never occurred at automobile low speed impacts and specifically relates to military high speed testing.

Table 13 – Test from Bolte et al. 2000 (padded tests), Compigne et al. 2004 (rigid tests), and Koh et al. (2005) [12] (rigid test) that induced AIS2+ injury at low deflections. All the deflection values were taken from Koh et al. (2005) [12] and are given non normalized.

	Test n° [ref]	Impactor features	2D acromion-to-T1 deflection peak value (mm)	Injuries
Padded tests	4009-L2 [7]	23 kg 4.23 m/s	35	· Distal clavicle (AIS 2) · Loose sternoclavicular
	6009-R1 [7]	23 kg 4.08 m/s	38	· Distal clavicle (AIS 2) · Loose sternoclavicular, loose acromioclavicular
	6009-L2 [7]	23 kg 4.55 m/s	31	· Distal clavicle (AIS 2) · Loose sternoclavicular, loose acromioclavicular
Rigid tests	LCE11 [9]	23.4 kg 6.07 m/s	34	· Distal clavicle (AIS 2) · Fracture at the base of the coracoid process (AIS 2) · Contusion of the inferior glenohumeral ligament
	LCE22 [9]	23.4 kg 4.27 m/s	39	· Acromion fracture at the junction of the scapula spine (AIS 2) · Fracture of the coracoid process extremity (AIS 2)
	#6 [12]	23.4 kg 4.51 m/s	36	· Distal clavicle fracture (AIS 2)

Limitations

First of all the general limitations of PMHS testing should be mentioned: the cadavers are generally old and lack muscle tone. This is an important difference compared to real soldier occupants in armoured vehicles.

The observations of the present study are limited by the low number of specimens tested. A larger test series including tests with higher impactor penetration would be required to confirm that humerus fracture is specific to IED blast impact and to determine if clavicle fracture can also occur.

The small size of the impactor surface may have favored the humerus fractures by inducing a bending-shearing of the diaphysis. The fact that the entire arm could not be pushed may have contributed to a concentrated load on the humeral head, inducing fractures even collapsing.

The supine posture of the subject may be a limitation but it is believed that it did not modify the results compared to a seated posture. In particular, constraining the back should be of negligible influence on the response because the penetration of the impactor did not exceed 50 mm and it was shown that only the shoulder extremity reacted during the impact.

Perspectives

The next step would be to develop a shoulder injury criterion using a lateral impact dummy that would be applicable to both the high speed-short penetration impact induced primarily by the IED blast and to the potential following impact due to the global motion of the military vehicle.

The force parameter would be considered rather than the deflection for two reasons. First, the ES-2re dummy is recommended by the NATO experts and it is not equipped with a shoulder deflection sensor. Second, the consistency of the PMHS deflection criterion is not established since the injury mechanism should be different between high speed-short duration and low speed-long duration impacts. A criterion based on the acromion deflection may be meaningless to explain humerus fractures.

Thus, the criterion would be based on the ES-2re shoulder force sensor. It is planned to consider both the magnitude and the duration in the future.

For that purpose, additional ES-2re dummy tests will be necessary to replicate the PMHS tests performed in the present study and those in the literature. Also, it may be necessary to conduct PMHS and ES-2re tests at an intermediate speed between 7 m/s and 27 m/s to help develop the criterion and finally to better define the injury risk curve.

V. CONCLUSIONS

A test set-up to allow delivering high speed (27 m/s)–short penetration (~4 cm) lateral impact to the shoulder was designed. The loading corresponded to the one of a deforming armored wall submitted to an IED blast.

Three AIS2 injurious PMHS tests were performed, all leading to humerus fractures. These injuries differed from the ones commonly found in lower speed impacts typical of the automotive field, for which the dominant AIS2 injury was the distal clavicle fracture. The resulting AIS2 injury correlated well with the peak force and the penetration into the skeleton.

The observation of the movies, the measurements and the injuries suggested a different injury mechanism than the one of the automobile field [12]. Little global motion of the body occurred during the impact. The upper arm and the shoulder joint were stamped by the impactor.

An injury criterion for such military impact using the ES-2re is still needed.

VI. ACKNOWLEDGEMENT

The authors of the present paper wish to acknowledge the LAB Renault PSA Peugeot Citroen, Nanterre, France, for having provided the test facilities, and in particular Erwan Lecuyer for his crucial part in obtaining the 100 kHz acquisition system. The efficiency of the CEESAR test team, Denis Dubois, Gilles Daniel and Catherine Potier, was also highly appreciated. Lastly, the authors wish to thank the scientists of the Wehrtechnische Dienststelle für Waffen und Munition (WTD 91), Meppen, Germany, for having shared the results of the ES-2re dummy full-size tests.

VII. REFERENCES

[1] RTO Technical Report HFM-090, "Test Methodology for Protection of Vehicle Occupants against Anti-Vehicular Landmine Effects. Final Report of HFM-090 Task Group 25". Internet: [http://www.cso.nato.int/abstracts.aspx], April 2007.

[2] RTO Technical Report HFM-148, "Test Methodology for Protection of Vehicle Occupants against Anti-Vehicular Landmine and/or IED Effects. Final Report of HFM-148". Internet: [http://www.cso.nato.int/abstracts.aspx], May 2012.

[3] STANAG 4569, "Protection levels for occupants of logistic and light armoured vehicles", Edition 1, NATO, 24 May 2004.

[4] Waßmuth E, Fucke W, Müller M, Hampel J, Dierkes U, German test and validation methodology of protection against asymmetric threats to armoured vehicles, *European Survivability Workshop*, 2008.

[5] Dierkes U, Müller M, Caylak V, Methods and Procedures for Investigation of Occupant Load in IED Road Side Blast Attacks, *European Survivability Workshop*, 2012.

[6] Charpail E, Trosseille X, Petit P, Laporte S, Lavaste F, Vallancien G, Characterization of PMHS Ribs: A New Test Methodology, *Stapp Car Crash Journal,* 49:183-198, 2005.

[7] Bolte IV J H, Hines M H, Mc Fadden J D, Saul R A, Shoulder response characteristics and injury due to lateral glenohumeral joint impacts, *Stapp Car Crash Journal*, 44:261-280, 2000.

[8] Bolte IV J H, Hines M H, Herriott R G, Mc Fadden J D , Donnelly B R, Shoulder impact response and injury due to lateral and oblique loading, *Stapp Car Crash Journal*, 47:35-53, 2003.

[9] Compigne S, Caire Y, Quesnel T, and Verries J-P, Non-injurious and injurious impact response of the human shoulder three dimensional analysis of kinematics and determination of injury threshold, *Stapp Car Crash Journal*, 48:89-123, 2004.

[10] Koh S W, Cavanaugh J M, Zhu J, Injury and Response of the Shoulder in Lateral Sled Tests, *Stapp Car Crash Journal,* 45:101-141, 2001.

[11] Marth D R, Biomechanics of the Shoulder in Lateral Impact, *Dissertation, Wayne State University, Detroit, USA*, 2002.

[12] Koh S W, Cavanaugh J M, Mason M J, Petersen S A, Marth D R, Rouhana S W, Bolte IV J H, Shoulder Injury and Response Due to Lateral Glenohumeral Joint Impact: An Analysis of Combined Data, *Stapp Car Crash Journal,* 49:291-322, 2005.

VIII. APPENDIX

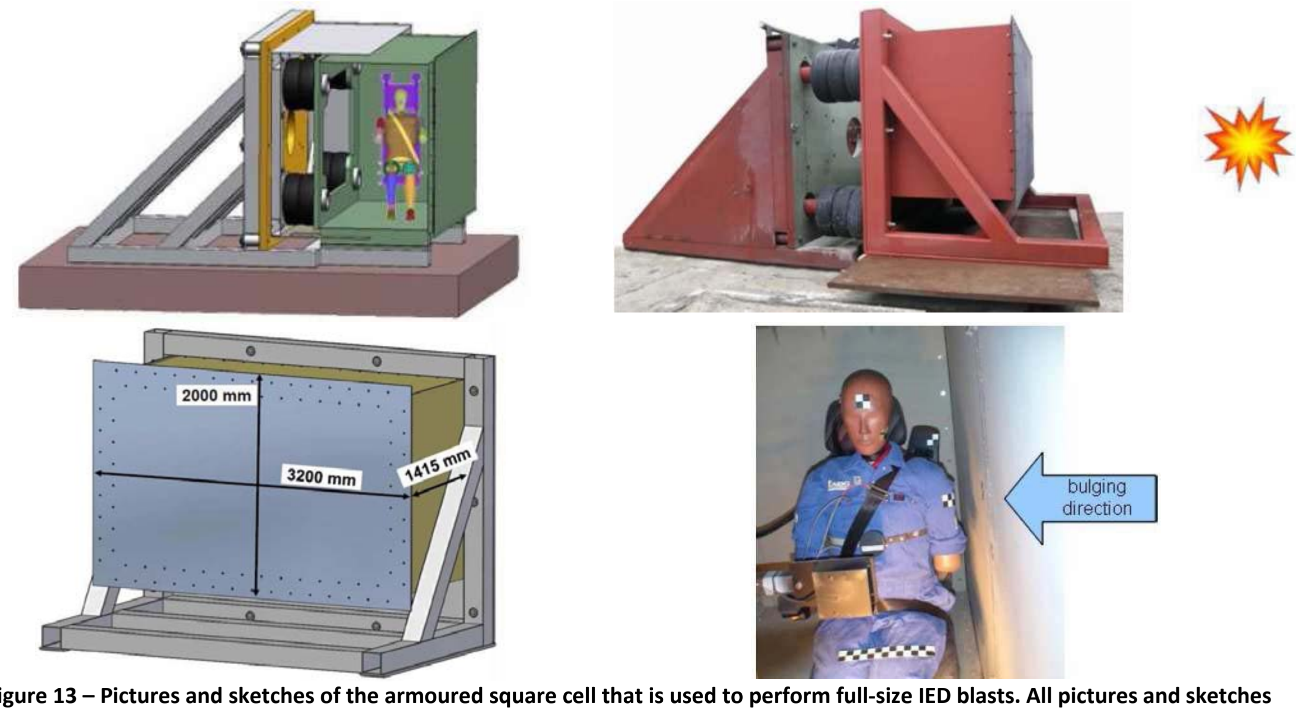

Figure 13 – Pictures and sketches of the armoured square cell that is used to perform full-size IED blasts. All pictures and sketches were taken from Dierkes et al. [5], except the bottom left sketch, which was kindly provided by the Wehrtechnische Dienststelle für Waffen und Munition, Meppen, Germany. The top left sketch shows the dummy posture inside the square cell. The top right picture shows at which side of the square cell the explosion is performed. The bottom right picture shows the resulting bulging direction of the side wall. The bottom left sketch shows the dimension of the deforming side wall.

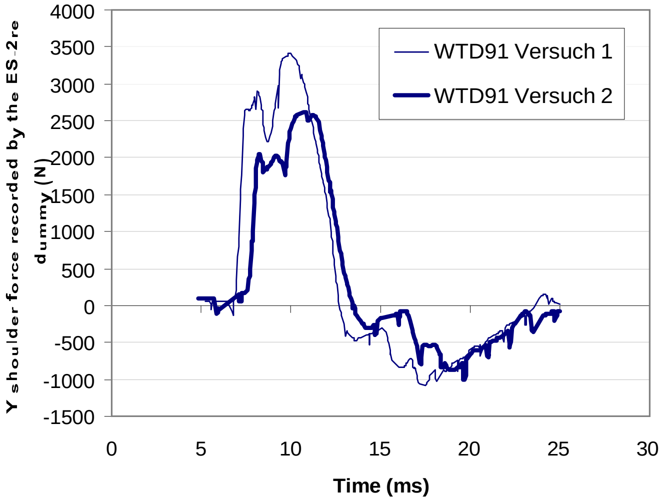

Figure 14 – Y shoulder force recorded by the ES-2re dummy during two experiments of full scale IED blast against the armoured cell described in Figure 13. For both tests (Versuch 1 and Versuch 2), the shoulder distance of the dummy with the side wall was 100 mm. This distance is called the stand-off. In test 1 (Versuch 1), the dummy only wear thin fabric clothes. In test 2 (Versuch 2) the dummy was equipped with a helmet and a bulletproof vest. The data were kindly provided by WTD91 (Wehrtechnische Dienststelle für Waffen und Munition, Meppen, Germany)

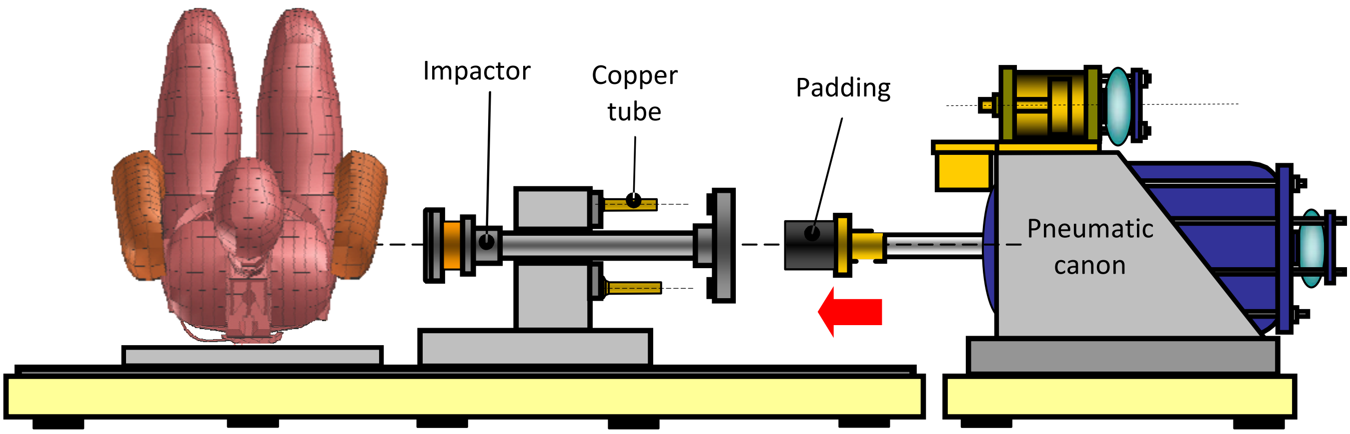

Figure 15 – Sketch of the whole test set-up. A pneumatic canon was used to propel the 7 kg-impactor at the speed of 27 m/s. With its 9 bar compressed air reservoir, it propelled a 19 kg-shaft at the speed 20 m/s. A padding was placed at the end of the shaft to mitigate the violence of the impact during the energy transmission with the impactor.

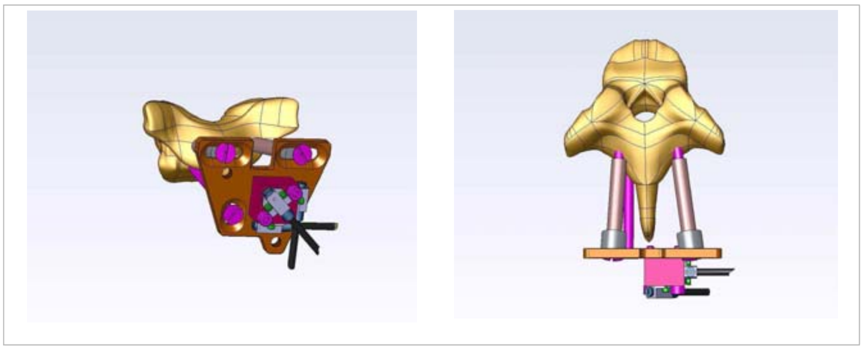

Figure 16 : accelerometers mount on T1 vertebra (back view at the left and upper view at the right). Three single-axis accelerometers are mounted on a cube. The cube is fixed to a plate. The plate is firmly attached to the T1 vertebral body using four screws.

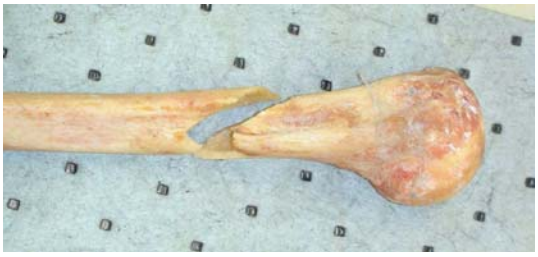

Figure 17: PCH2070 – Anterior view of the upper part of the humerus.

Figure 18: PCH2070 – Posterior view of the upper part of the humerus.

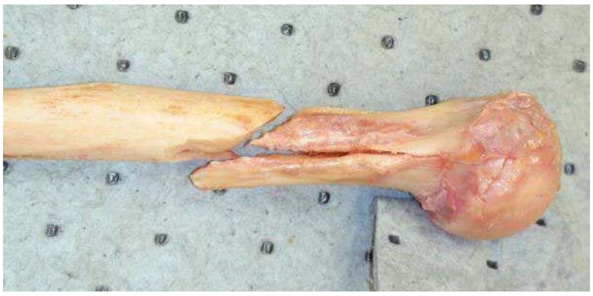

Figure 19. PCH2074 – Anterior view of the upper part of the humerus

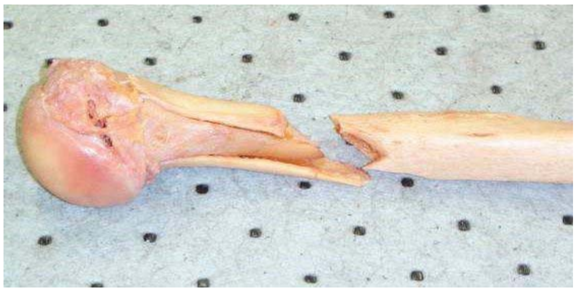

Figure 20. PCH2074 – Posterior view of the upper part of the humerus

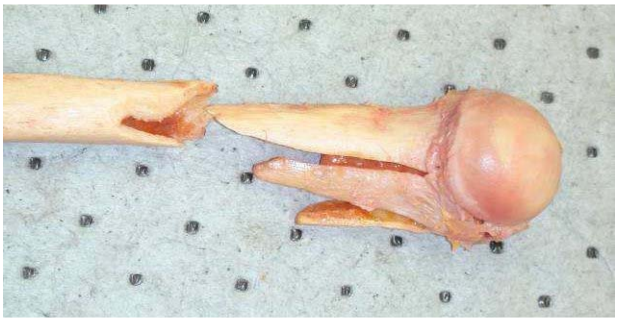

Figure 21. PCH2074 – Medial view of the upper part of the humerus

Figure 22. PCH2074 – Superior view of the humeral head

Table 14 – Parameters, which were cross-plotted with the TAIS 2005 in Figure 12, and acromion deflection estimator, which was computed according to the procedure described in Table 12.

PMHS n°	Test n°	TAIS 2005	Max. body reaction force (N)	Max. total deflection (mm)	Max. total compression (%)	Max. skeletal deflection (mm)	Max. skeletal compression (%)	Max. skeletal penetration (mm)	Acromion deflection estimator (mm)
643-L	PCH2069	1	6.6	-31	15%	-18	9%	-19	-12
643-R	PCH2070	5	10.3	-43	21%	-26	12%	-26	-17
644-L	PCH2071	1	5.8	-36	19%	-16	8%	-16	-5
644-R	PCH2072	1	7.0	-41	22%	-16	8%	-16	-4
645-L	PCH2073	13	11.5	-48	23%	-30	14%	-32	-27
645-R	PCH2074	8	10.4	-39	18%	-24	11%	-26	-15
Mean		5	8.6	-40	20%	-22	11%	-23	-14
SD		5	2.4	6	3%	6	3%	6	8

Figure 23. PCH2073 – Anterior view, fracture of the coracoid process base and, following, the fracture of the supraspinatus fossa

Figure 24. PCH2073 – Anterior view, Coracoid process after detachment

Figure 25. PCH2073 – Superior view, acromion fracture drawn in blue

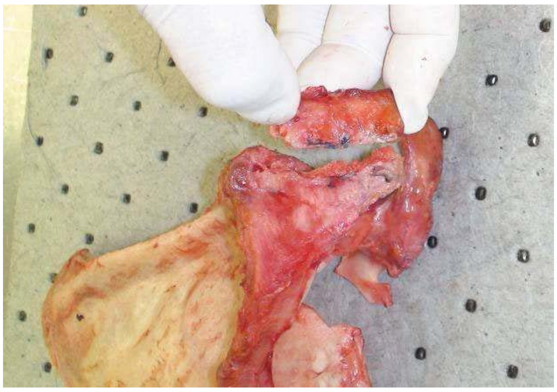

Figure 26. PCH2073 – Superior view, acromion fracture after detachment

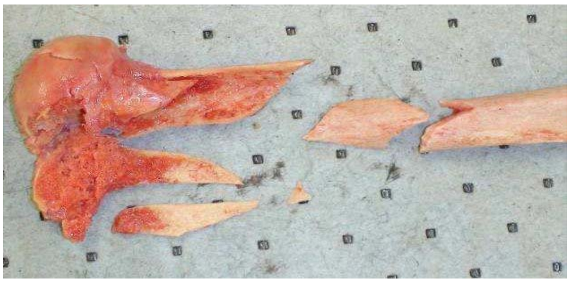

Figure 27. PCH2073 – Posterior view of the upper part of the humerus

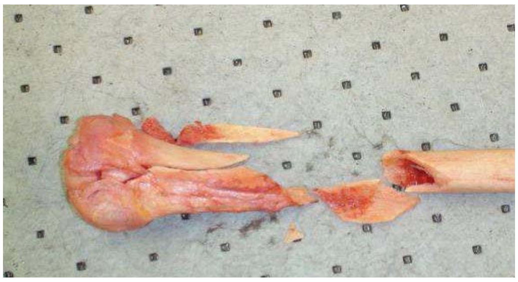

Figure 28. PCH2073 – Anterior view of the upper part of the humerus

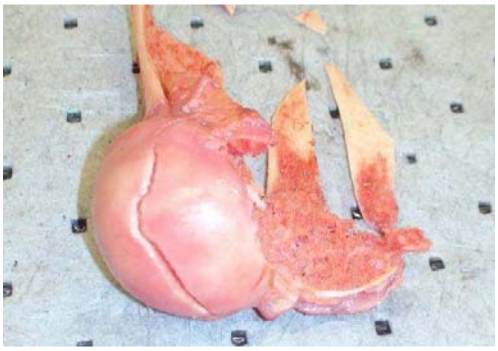

Figure 29. PCH2073 – View of the humeral head

Figure 30. PCH2073 – View of the humeral head

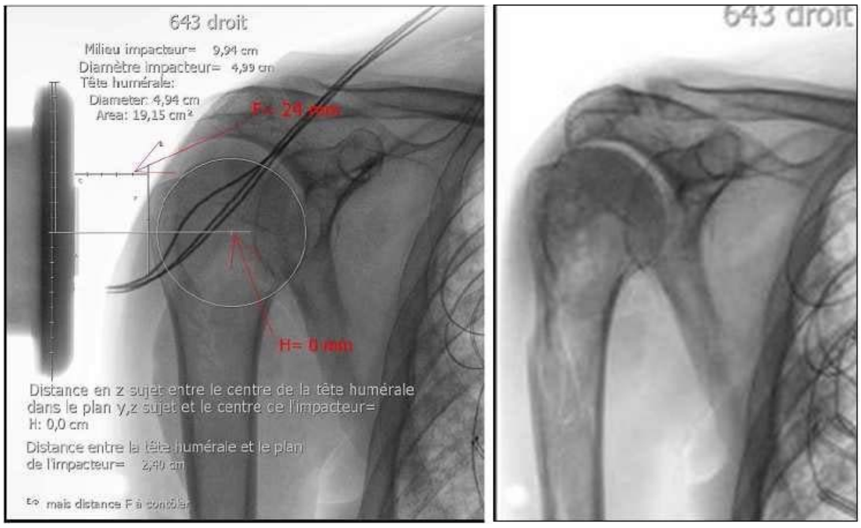

Figure 31 – Test PCH2071, PMHS 643: Pre-test (left) and post-test (right) face view X-rays of the right shoulder

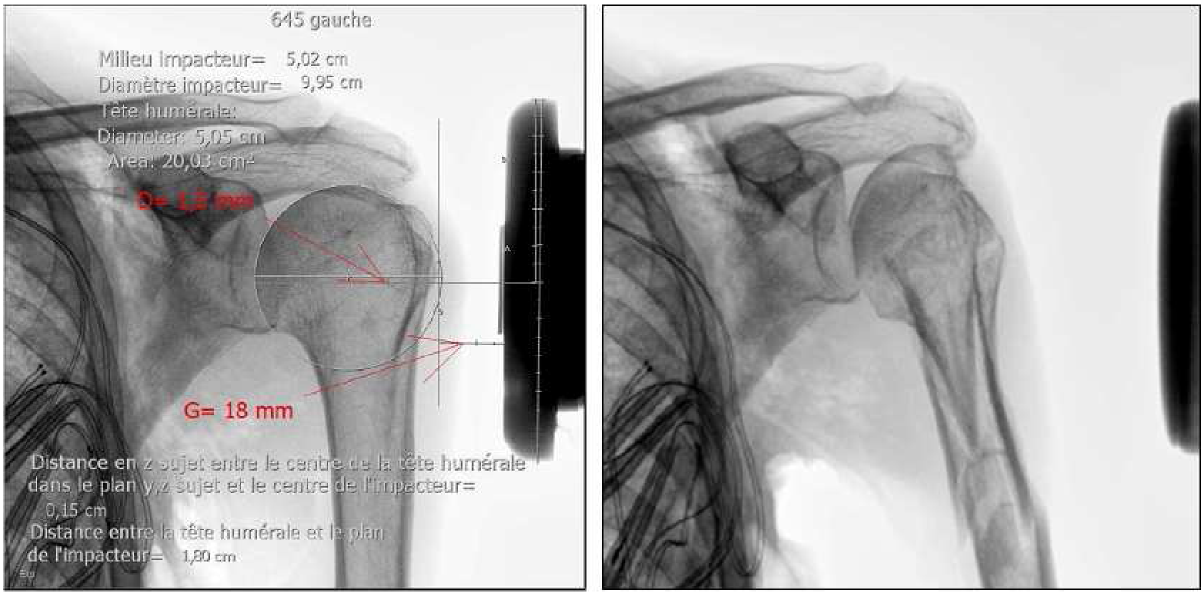

Figure 32 – Test PCH2073, PMHS 645: Pre-test (left) and post-test (right) face view X-rays of the left shoulder

Figure 33 – Test PCH2074, PMHS 645: Pre-test (left) and post-test (right) face view X-rays of the right shoulder